Focused on Crack Tip Fields

A model to quantify fatigue crack growth by cyclic damage accumulation calculated by strip-yield procedures

Samuel Elias Ferreira, Jaime Tupiassú Pinho de Castro, Marco Antonio Meggiolaro
Pontifical Catholic University of Rio de Janeiro, PUC-Rio, R. Marquês de São Vicente 225, Rio de Janeiro, 22451-900, Brazil
ferreirase@hotmail.com, jtcastro@puc-rio.br, meggi@puc-rio.br

ABSTRACT. Elber's hypothesis that ΔK_{eff} can be assumed as the driving force for fatigue crack growth (FCG) is the basis for strip-yield models widely used to predict fatigue lives under variable amplitude loads, although it does not explain all load sequence effects observed in practice. To verify if these models are indeed intrinsically better, the mechanics of a typical strip-yield model is used to predict FCG rates based both on Elber's ideas and on the alternative view that FCG is instead due to damage accumulation induced by the cyclic strain history ahead of the crack tip, which does not need or use ΔK_{eff} ideas. The main purpose here is to predict FCG using the cyclic strains induced by the plastic displacements calculated by strip-yield procedures, assuming there are strain limits associated both the with the FCG threshold and with the material toughness. Despite based on conflicting principles, both models can reproduce quite well FCG data, a somewhat surprising result that deserves to be carefully analyzed.

KEYWORDS. Fatigue crack growth models; Strip-yield mechanics; Crack closure; Damage accumulation ahead of the crack tip.

OPEN ACCESS

Citation: Ferreira, S.E., Castro, J.T.P., Meggiolaro, M.A., A model to quantify fatigue crack growth by cyclic damage accumulation calculated by strip-yield procedures, Frattura ed Integrità Strutturale, 41 (2017) 129-138.

Received: 28.02.2017
Accepted: 15.04.2017
Published: 01.07.2017

INTRODUCTION

Paris and Erdogan clearly demonstrated that stable fatigue crack growth (FCG) rates da/dN can be correlated to stress intensity factor (SIF) ranges ΔK, at least in the central region of typical $da/dN \times \Delta K$ curves, where theirs $da/dN = A \cdot \Delta K^m$ rule applies [1]. Following their idea, many others proposed similar rules to consider the effects of other parameters that can affect FCG rates as well, such as the peak load K_{max} or the load ratio $R = K_{min}/K_{max}$, FCG thresholds $\Delta K_{th}(R)$, and the toughness K_C [2]. In particular, after discovering crack closure under tension loads, Elber postulated that additional fatigue damage could only be induced after the crack tip is fully opened under loads greater than K_{op}, the crack opening load [3-4]. His $da/dN = f(\Delta K_{eff} = K_{max} - K_{op}$ if $K_{op} > K_{min})$ hypothesis can plausibly explain many characteristics of the fatigue cracking behavior, such as FCG delays and arrests induced by overloads (OL), reductions on OL-induced delays after underloads (UL), or the existence of R-dependent FCG thresholds, which can very much affect fatigue lives under variable amplitude loads (VAL). The ΔK_{eff} idea has been used since then in many semi-empirical FCG models, among them the strip-yield models (SYM) that estimate K_{op} and FCG lives using a suitable $da/dN \times \Delta K_{eff}$ rule properly fitted to experimental data [5-9].

Works that support the $da/dN = f(\Delta K_{eff})$ hypothesis are extensively reviewed e.g. by Kemp [10] and by Skorupa [11-12], but many other works question it. FCG delays or arrests after OLs under high R while the crack remains fully opened, always maintaining $K_{min} > K_{op}$ [13]; constant FCG rates induced by fixed $\{\Delta K, R\}$, but highly variable ΔK_{eff} loadings [14-15]; cracks arrested at a given R that restart to grow at a lower R under the same ΔK_{eff} [16]; or the R-insensibility of FCG in inert environments [17], are examples of FCG behaviors that cannot be explained by Elber's postulate. Although this work does not aim to support or to refute Elber's idea, neither to review the works that support or question it, it can be claimed that there is no doubt it still remains controversial.

In view of such doubts, this work first uses well-proved strip-yield mechanics [5-9] to model some $da/dN \times \Delta K$ curves measured at low and high R. However, instead of just assuming that a reasonable description of some fatigue data confirms that the ΔK_{eff} hypothesis is valid, the very same mechanics is then used to verify if the same data can be equally described by the alternative view that FCG, instead of controlled by ΔK_{eff}, is due to damage accumulation ahead of the crack tip. This critical damage model (CDM) assumes that fatigue cracks grow by sequentially breaking small volume elements (VE) adjacent to the crack tip after they reach the critical damage the material can sustain. If properly applied, this alternative idea do not need the ΔK_{eff} hypothesis or requires arbitrary data-fitting parameters [13, 18-20].

FCG MODELS

Four FCG models are studied following: (i) the critical damage model (CDM) proposed in [18-20]; (ii) a strip-yield model (SYM) based on [6]; (iii) a combination of the strip-yield with the critical damage model (SYM-CDM) using fracture mechanics tools; and (iv) a modified strip-yield critical damage model (mod SYM-CDM) proposed here.

Fig 1 illustrates the CDM principles that allow the use of εN concepts, used to describe fatigue crack initiation, to model FCG as well. This simple model basically assumes that: (i) fatigue cracks grow by successively breaking small VE located ahead of their tips; (ii) such VE can be treated as tiny εN specimens fixed along the crack path; (iii) these VE accumulate fatigue damage induced by variable strain ranges, which increase as the crack tip approaches them; and (iv) the fracture of the VE adjacent to the crack tip occurs because it accumulated the entire damage the material can tolerate.

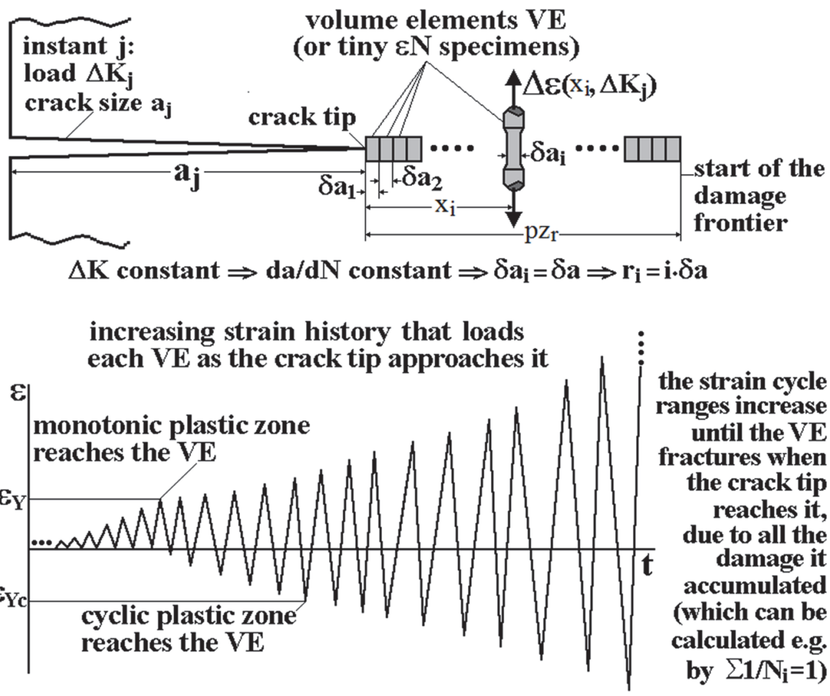

Figure 1: Schematics of the FCG process caused by successive fractures of the VE adjacent to the crack tip at every load cycle [2].

Since constant amplitude SIF range induce constant FCG rates, the VE widths in such cases can also be assumed fixed and equal to the crack increment per cycle. Any given VE suffers damage in each load cycle, caused by the strain loop range induced by that cycle, which depends on the distance x_i between the i-th VE and the fatigue crack tip (Fig. 1). The strain ranges acting in any given VE increase at every load cycle, as the crack tip approaches it. The fracture of the VE adjacent to the crack tip occurs when its accumulated damage reaches a critical value, estimated by the linear damage accumulation rule (or by any other suitable damage accumulation rule) as:

$$\sum_i \left[n_i / N_i(x_i) \right] = 1 \tag{1}$$

where $N_i(x_i)$ is the number of cycles that the i^{th} VE located at a distance x_i from the crack tip would last if only that cycle loading would act during its whole life, and n_i is the number of cycles that acted at that load, in this case just one.
The CDM uses the elastoplastic strain distribution ahead of the crack tip to calculate damage in every VE. However, like in the LE case, EP models for the stress and strain fields inside the plastic zones pz ahead of a crack tip assumed to have a zero tip radius $\rho = 0$, like the HRR field [21-22], are singular at $x = 0$ as well. To eliminate this undesired and physically inadmissible feature (since no loaded cracks can sustain infinite strains at their tips), the necessarily finite EP stress and strain fields can be estimated by shifting the HRR field origin into the crack by a distance X. This procedure is inspired by Creager and Paris' idea originally used to estimate stress concentration factors K_t from the SIF of geometrically similar cracks [23]. Under constant SIF range conditions the crack advances a distance equal to the VE width in each cycle ($n_i = 1$), so the sum in Eq. (1) can be approximated by an integral along, say, the reverse or cyclic plastic zone (pz_r), neglecting in a first approximation fatigue damage induced outside it:

$$\frac{da}{dN} = \int_0^{pz_r} \frac{dx}{N\left(x + X\right)} \tag{2}$$

The HRR field origin shift can be estimated e.g. assuming $X = \rho/2$, as Creager and Paris did, where ρ is the (finite) crack tip radius under the peak load K_{max}. To calculate the cyclic plastic strain range $\Delta\varepsilon_p$ ahead of the crack tip, the modification proposed by Schwalbe [24] can be used as in [19]:

$$\Delta\varepsilon_p\left(x + X\right) = \left(2S_{Yc}/E\right) \cdot \left[pz_r / \left(x + X\right) \right]^{1/\left(1+h_c\right)} \tag{3}$$

where S_{Yc} is the cyclic yield strength of the material, E is its Young's modulus, and h_c is its Ramberg-Osgood strain-hardening exponent. Since the elastic strain amplitude inside the cyclic plastic zone is neglected in Eq. (3), its associated fatigue life $N(x + X)$ can be estimated from the plastic part of Coffin-Manson's equation by

N,x+X.=,1-2.,,,Δ,ε-p.(x+X)-2,ε-c...-,1-c.. (4)

where c and ε_c are Coffin-Manson's plastic exponent and coefficient, respectively. Hence, estimating the X displacement of the modified HRR field in the same way as Creager and Paris did with the LE Williams field, i.e. assuming it as $\rho = CTOD/2$, where $CTOD$ is Schwalbe's estimate for the Crack Tip Opening Displacement induced by K_{max}, then

$$X = \frac{\rho}{2} = \frac{CTOD}{4} = \frac{K_{max}^2 \cdot \left(1 - 2\nu\right)}{\pi \cdot E \cdot S_{Yc}} \cdot \sqrt{\frac{1}{2\left(1 + h_c\right)}} \tag{5}$$

The FCG rate induced by constant SIF ranges, i.e. by fixed $\{\Delta K, R\}$ conditions, can then be estimated by Eq. (2)-(5). Finally, these resulting da/dN values can be used to calculate the constant C in a modified McEvily's rule that simulates all 3 phases of typical $da/dN{\times}\Delta K$ curves, considering the FCG threshold ΔK_{th} and the toughness K_c limits in FCG rates:

$$da/dN = C \cdot \left(\Delta K - \Delta K_{th}\right)^2 \cdot \left[K_c / \left(K_c - K_{max}\right) \right] \tag{6}$$

Another less arbitrary and probably more reasonable way to estimate the X displacement of the HRR field origin (needed to remove the strain singularity at the crack tip) uses the strains induced by K_{max} at the crack tip predicted by a suitable strain concentration rule, as described in [19]. In any way, the whole $da/dN \times \Delta K$ curve can be estimated using only well-defined materials properties, without the need for any data-fitting parameter. Such equations describe the simplest formulation of this CDM, since they apply only to constant SIF range conditions, but this model can be further developed to describe FCG under VAL as well, see [20].

Strip-yield models, on the other hand, numerically estimate the K_{op} needed to find ΔK_{eff} using the classic Dugdale-Barenblatt's idea [25-26], modified to leave a wake of plastically deformed material around the faces of the advancing fatigue crack. Dugdale's model estimates the plastic zone size in a Griffith plate of an elastic perfectly plastic material under plane stress (pl-σ) conditions, assuming the pz formed ahead of both crack tips under a given K_{max} work under a fixed tensile stress equal to the material yield strength S_Y (neglecting strain-hardening and stress gradients inside the pz).

There are several algorithms based on these ideas [5-9]. The SYM algorithm implemented in this work is based in Newman's original work [6], but it uses the FCG rule and material parameters specified as in the NASGRO code [27]. The validation of this home-made algorithm was performed by comparing its opening stress predictions under several load conditions with results from the literature [28-29]. Newman's original SYM calculates pz sizes and surface displacements by superposition of two LE problems: (i) a cracked plate loaded by a remote uniform nominal tensile stress and, (ii) a uniform stresses distributed over surface segments near the crack tip.

Fig 2 schematizes the crack surface displacements and the stress distributions around the crack tip at the maximum and minimum loads σ_{max} and σ_{min}. The plastic zones and the crack wakes left by previous cycles are discretized in a series of rigid-perfectly-plastic 1D bar elements, which are assumed to yield at the flow strength of the material, $S_{FL} = (S_Y + S_U)/2$, to somehow account for the otherwise neglected strain-hardening effects – a first order approximation. These elements are either intact at the plastic zone or broken at the crack wake, keeping residual plastic deformations. If they are in contact, the broken bar elements can carry compressive stresses, and they can yield in compression when their stresses reach $-S_{FL}$. The elements along the crack face that are not in contact do not affect the crack surface displacements, neither carry stresses.

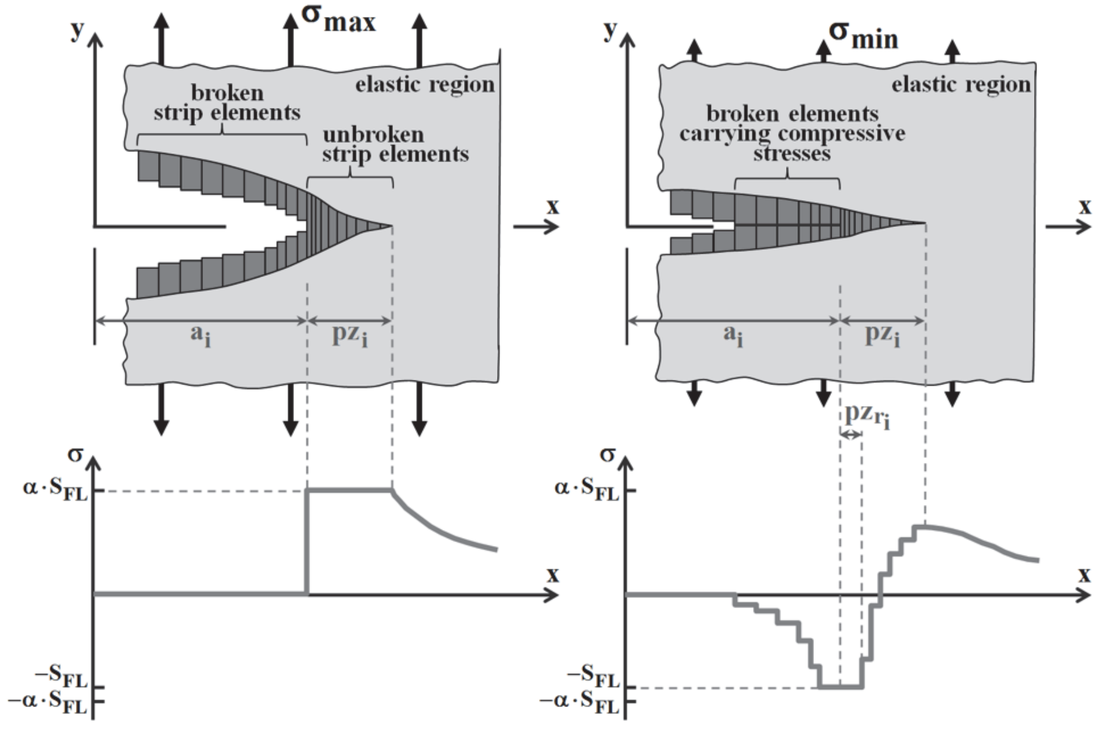

Figure 2: Crack surface displacements and stress distribution along the crack line according to the SYM [6].

It is important to somehow consider the effects of the actually 3D stresses around the crack tip, caused by transversal plastic restrictions induced by the high strain gradients that act there when the plate is thick and cannot be assumed to work under limiting pl-σ conditions. To do so in the 1D SYM, it uses a thickness-dependent constraint factor α to

increase the tensile flow stress S_{FL} in the unbroken elements along the plastic zone during the loading. Hence, this constraint factor should vary from $\alpha = 1$ for plane stress conditions in thin plates, to up to $\alpha = 1/(1-2\nu) \cong 3$ for plane strain limit conditions in thick plates, where ν is Poisson's coefficient (but in practice it is often used as an additional data-fitting parameter). Since there is no crack-tip singularity when the crack closes, this constraint factor is not used to modify the compressive yield strength during unloading, assuming the conditions around the crack tip tend to remain uniaxial.
Eq. (7) presented below governs the SYM behavior by requiring compatibility between the LE part of the cracked plate and all bar elements along the crack surfaces and inside the *pz* ahead of the crack tip. When the length of the wake elements L_j is larger than their displacement V_j under σ_{min}, they contact and induce a stress σ_j needed to force $V_j = L_j$. The influence functions $f(x_i)$ and $g(x_i, x_j)$ used in Eq. (7) are related to the plate geometry and its width correction, and are calculated like described in [6].

$$V_i = \sigma_n \cdot f(x_i) - \sum_{j=1}^{n} \sigma_j \cdot g(x_i, x_j) \tag{7}$$

To improve the resolution of the SYM used here, the *pz* ahead of the crack tip is divided into 20 bar elements, or twice the number of elements used in the original Newman's model [6]. After calculating the *pz* size induced by the peak stress σ_{max} applied in the current cycle, the widths of the bar elements inside the plastic zone are calculated by Eq. (7), replacing the terms n by 20 and σ_j by $\alpha \cdot S_F$, see Fig. 2a.
When the plate is unloaded to the minimum load σ_{min} (Fig. 2b), the bar elements inside the *pz* are also unloaded until some of them near the crack tip start to yield in compression, because they try to reach a stress $\sigma_j \leq -S_F$. The size of this reverse plastic zone pz_r depends on the amount of crack closure and on the transversal constraints induced by the plate thickness. The broken elements located inside the plastic wake formed along the crack surfaces, which store residual deformations, may come into contact and carry compressive stresses as well. Some of these elements may also yield in compression, if they try to reach $\sigma_j \leq -S_F$. The stresses σ_j at each of the *n* elements inside the plastic zone and along the plastic wake that surrounds the crack surfaces are calculated solving the system of equations from Eq. 7 using $V_i = L_i$ (at σ_{max}) and $\sigma_n = \sigma_{min}$. Crack opening loads and residual plastic deformations are calculated considering contact stresses.
During the crack propagation stage, the opening stress is kept constant during a small arbitrary crack increment to save computer cost. The number of load cycles ΔN required to grow the crack by this increment is calculated by by Eq. (8) [27], in which the parameters C_n, m, p and q are data-fitting constants, K_c is the material toughness, and the FCG threshold ΔK_{th} can be estimated using a procedure described in [27].

$$da/dN = C_n\left(\Delta K_{eff}\right)^m \cdot \left(1-\Delta K_{th}/\Delta K\right)^p \Big/ \left(1-K_{max}/K_c\right)^q \tag{8}$$

The combination of CDM with SYM procedures uses the same strip-yield description adopted by the SYM to calculate the plastic strain ranges and the consequent fatigue damage distribution ahead of the crack tip. This replace the displaced HRR strain field used by the original critical damage model [19]. This model estimates the FCG increments in a cycle-by-cycle basis by a gradual damage accumulation process, but considering possible crack closure effects on the cyclic strain field ahead of the crack tip. The *pz* ahead of the crack tip is divided into small bar elements with constant width, whose quantity varies between 150 and 550, depending on the loading conditions. The plastic displacements within the SYM strip-yield are transformed into plastic strains using a solution proposed by Rice [30] to estimate the strain field based on CTOD variations, properly modified to consider each bar element displacements by

$$\Delta\varepsilon_y(i) = log\left[\left(2L_{max}(i) + x_{ct}(i)\right)\Big/\left(2L_{min}(i) + x_{ct}(i)\right)\right] \tag{9}$$

The displacements L_{max} and L_{min} of the i^{th} element inside the *pz* are calculated at the maximum and minimum applied stresses. The position of the elements starting from the crack tip, $x_{ct}(i)$, is located at the center of each element. The strain range $\Delta\varepsilon_y$ that acts at each element center can be correlated to the number of cycles that would be required to break that element by the plastic part of Coffin-Manson's rule (C&M) Eq. (10), or else by SWT rule Eq. (11), to consider peak stress effects. Notice that only the plastic part of the strain range can be considered by this SY-CDM, because the strain ranges estimated from the SYM displacements are calculated assuming rigid-perfectly-plastic bar elements. The total damage accumulated by each element is evaluated by Palmgren-Miner's rule Eq. (1).

$$N(i) = (1/2)\left(\Delta\varepsilon_y(i)/2\varepsilon_c\right)^{1/c} \tag{10}$$

$$N(i) = (1/2)\left(\sigma_{\max}(i)\cdot\Delta\varepsilon_y(i)/2\sigma_c\varepsilon_c\right)^{1/(b+c)} \tag{11}$$

Since the numerical model calculates fatigue damage at the central position of each VE, the crack increment induced by each load cycle is given by the location where the damage reaches one ahead of the crack tip. Therefore, the damage value of the new first element are calculated using a linear interpolation procedure. As the number of elements is unchanged, to keep the width sum of all elements equal to the *pz* size, the first and the last element can have a variable width. Moreover, since Eq. (6) reproduces the sigmoidal shape of $da/dN\times\Delta K$ curves, and since its only adjustable constant C can be directly calculated for any $\{\Delta K, R\}$ combination from the εN properties of the material, the CDM used here in fact have no data-fitting parameters (whereas the NASGRO FCG rule used at the SYM needs 4 of them). The C constant (Eq. 6) is found using several da/dN values calculated by SY-CDM procedures using C&M or SWT rules. This process is similar to the adopted by the original CDM. The main difference here is the replacement of a shifted HRR strain field by a strain field derived from the displacement field of the SYM.

The new modification proposed here for the SY-CDM eliminates the need of assuming that the da/dN versus ΔK curve of the material is always described by McEvily's rule Eq. (6). This can be achieved by assuming two new hypotheses, which are also based on the physics of the FCG process. The first supposes that there is a limit strain range below which the crack does not grow by fatigue, which is directly related to the SIF range threshold ΔK_{th}. The second assumes the crack becomes unstable at a maximum plastic strain related to the critical stress intensity factor, or to the material toughness. These hypotheses are described by:

$$\Delta\varepsilon_{y,\mathrm{mod}}(i) = \left[\Delta\varepsilon_y(i) - \Delta\varepsilon_{y,th}(i)\right]\cdot\left[\varepsilon_{y,cr}(i)/\left(\varepsilon_{y,cr}(i) - \varepsilon_{y,\max}(i)\right)\right] \tag{12}$$

The plastic strain range calculated by Eq. (12) is used by the modified SY-CDM to calculate the damage at each element by Eq. (10) or (11). The interpolation routine was improved to work with a fixed number of elements (400) for any load condition and, due these hypotheses, one less step is required to estimate the FCG Finally, a major fringe-benefit of all CDMs used in this work must be emphasized: if they can reasonably estimate FCG rates for a given material, they do so using *only* its εN, ΔK_{th}, and K_C properties, without the need for any adjustable data-fitting parameters. Therefore, these simple and sound models can indeed be called *predictive*, since they do not need or use actual FCG data points to estimate da/dN rates. The results presented next support this claim.

EXPERIMENTAL RESULTS AND DISCUSSIONS

These four models are compared against experimental $da/dN\times\Delta K$ data measured at $R = 0.1$ and $R = 0.7$ for two materials, a 7075-T6 Al alloy and a 1020 low carbon steel, as described elsewhere [19]. These materials properties and the C values used by the C&P CDM (model i) are listed in Tab. 1. FCG rates predictions by the SYM (model ii) use material properties from NASGRO version 4.02, as shown in Tab. 2. But instead of using Poisson's coefficients to estimate the constraint factor α, its value was varied to verify its effect on FCG predictions. Values $\alpha = 3$ for 7075 and $\alpha = 2$ for the 1020 resulted in good approximations and are adopted here. The $\Delta K_{th}(R)$ and K_{IC} from Tab. 1 are used in Eq. 8, since they approximate the data better than the values listed in NASGRO. The constants C from Eq. (6), model (iii), are listed in Tab. 3.

Material	S_Y (MPa)	S_U (MPa)	σ_c (MPa)	ε_c	b	c	K_{IC} (MPa√m)	ΔK_{th} (MPa√m)		C (for ΔK in MPa√m)
								R = 0.1	R = 0.7	
7075-T6	498	576	709	0.12	-0.056	-0.75	25.4	3.4	2.9	8.23e-09
1020	285	491	815	0.25	-0.114	-0.54	277	11.6	7.5	2.73e-10

Table 1: Material properties [19] and C values obtained by several strain concentration rules.

Material	S_Y (MPa)	S_U (MPa)	C_n (for ΔK in MPa√mm	m	p	q
7075-T6 (M7HA03AB1)	461.9	524	$9.686 \cdot 10^{-12}$	3	0.5	1
1015-1026 (C1BB11AB1)	262	399.9	$1.515 \cdot 10^{-14}$	3.7	0.5	0.5

Table 2: Properties and Forman-Newman parameters from the NASGRO 4.02 database [27].

εN equation	C (for ΔK in MPa√m)	
	7075-T6	1020
C&M	8.73e-09	2.64e-09
SWT	1.49e-08	4.50e-09

Table 3: Constant C for modified CDMs obtained from SYM-calculated cyclic strain fields.

Figs. 3 and 4 show the measured $da/dN \times \Delta K$ points and the curves predicted by the original CDM based on Creager and Paris (C&P), by the original SYM (assuming $\alpha = 3$), by the SY-CDMs (SY-C&M and SY-SWT), and also by the modified SY-CDMs proposed here (SY-C&M modified and SY-SWT modified). The FCG data has been obtained under $R = 0.1$ and $R = 0.7$ using standard ASTM E647 procedures for a 7075-T6 Al alloy and a 1020 steel, respectively. Recall that the SY-CDM curves are predicted from the εN damage induced by the cyclic strain fields generated by SYM strip-yield procedures using Coffin-Manson or STW εN rules. These models use only the plastic part of those εN rules because the SYM numerical procedures discretize the pz ahead of the crack tip using rigid-perfectly-plastic VE elements. Recall as well that the modified SY-CDM proposed here does not need to use a previously chosen $da/dN \times \Delta K$ rule (Eq. 6) due the two limiting strain values introduced in the model, one for the FCG threshold and the other for the toughness.

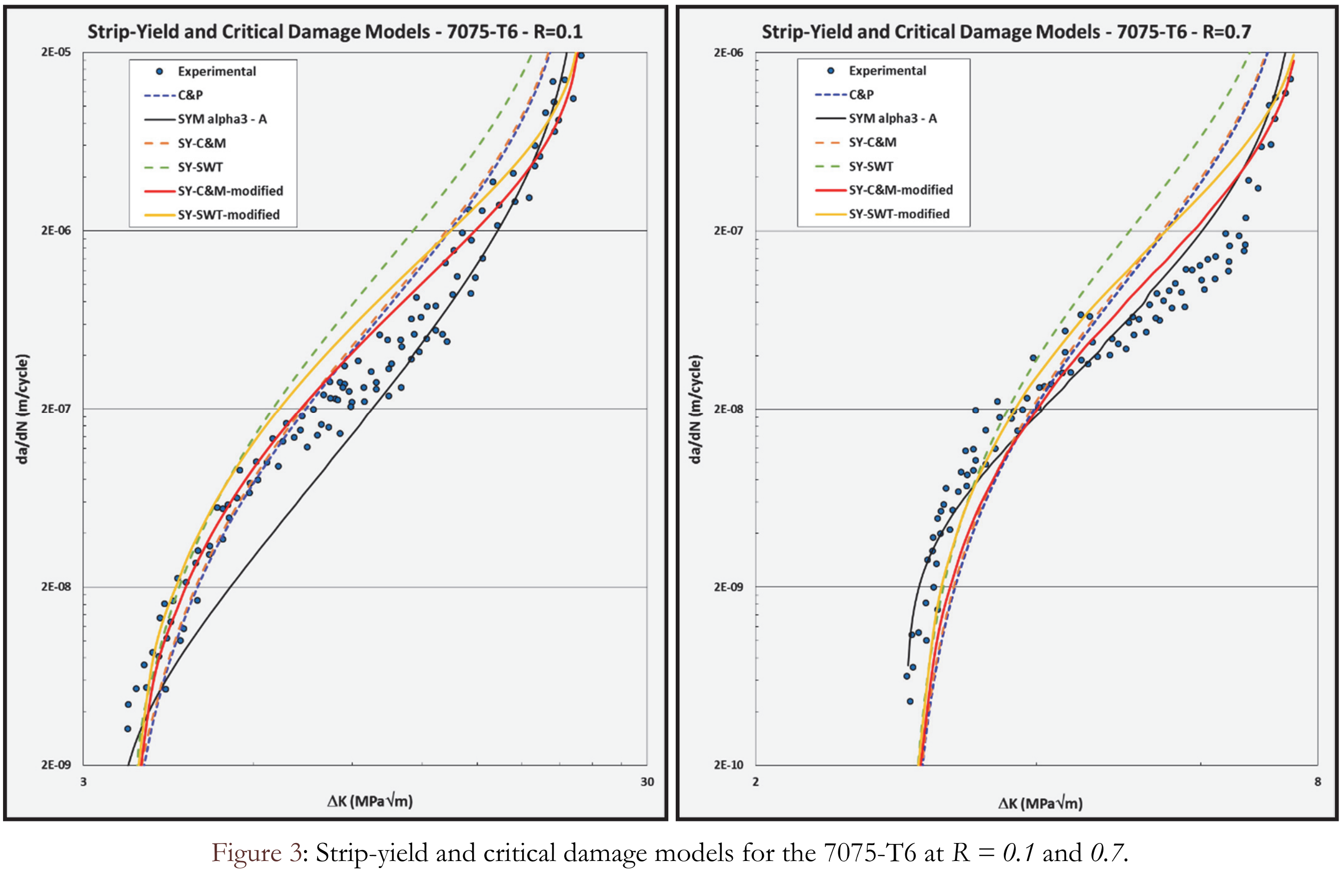

Figure 3: Strip-yield and critical damage models for the 7075-T6 at R = 0.1 and 0.7.

Notice in Fig. 3 that the $da/dN \times \Delta K$ curve estimated by the SY-C&M model is essentially equal to the curve generated by the original C&P CDM model. Both estimates are quite reasonable for $R = 0.1$, albeit not as good for $R = 0.7$. The SYM curve (generated assuming $\alpha = 3$) describes better the data points measured at $R = 0.7$. The SWT εN model estimates higher FCG rates than the C&M model for both R-ratios, as expected. The model proposed here (SY-C&M-modified, which does not need an assumed FCG rule) yielded the best estimates at $R = 0.1$ and had a performance similar to the SYM at $R = 0.7$.

The modified SY-CDMs had in particular a better performance at the higher ΔK ranges, where the original models systematically estimated FCG rates higher than the data. The original CDM [19] and SY-CDM models need a pre-chosen McEvily'-type $da/dN \times \Delta K$ curve, whose single adjustable parameter can however be calculated by εN procedures. Their good performance certainly is not a coincidence, since they use no adjustable data-fitting parameters and their predictions are entirely based on measured εN properties. In fact, when compared to SYM estimates based on ΔK_{eff} concepts and on a FCG rule that has 4 adjustable data-fitting parameters, not to mention the constraint factor α that in practice is frequently used as a 5th adjustable parameter, the CDM performance could be even qualified as quite impressive for a so simple model.

The results for the 1020 steel are shown in Fig. 4. The original CDM based on a Creager and Paris shift of the HRR field reproduced well the data trend, but yielded slight non-conservative FCG estimates at $R = 0.1$. For $R = 0.7$ it presented a still better performance. The original SYM had a similar performance at $R = 0.1$, but instead generated slight conservative predictions, which deviated from data at low ΔK values. For $R = 0.7$ its predictions were not good. The modified SY-C&M generated quite reasonable predictions for $R = 0.7$, but for $R = 0.1$ they were maybe too conservative. The other models yielded too conservative predictions for both R-ratios.

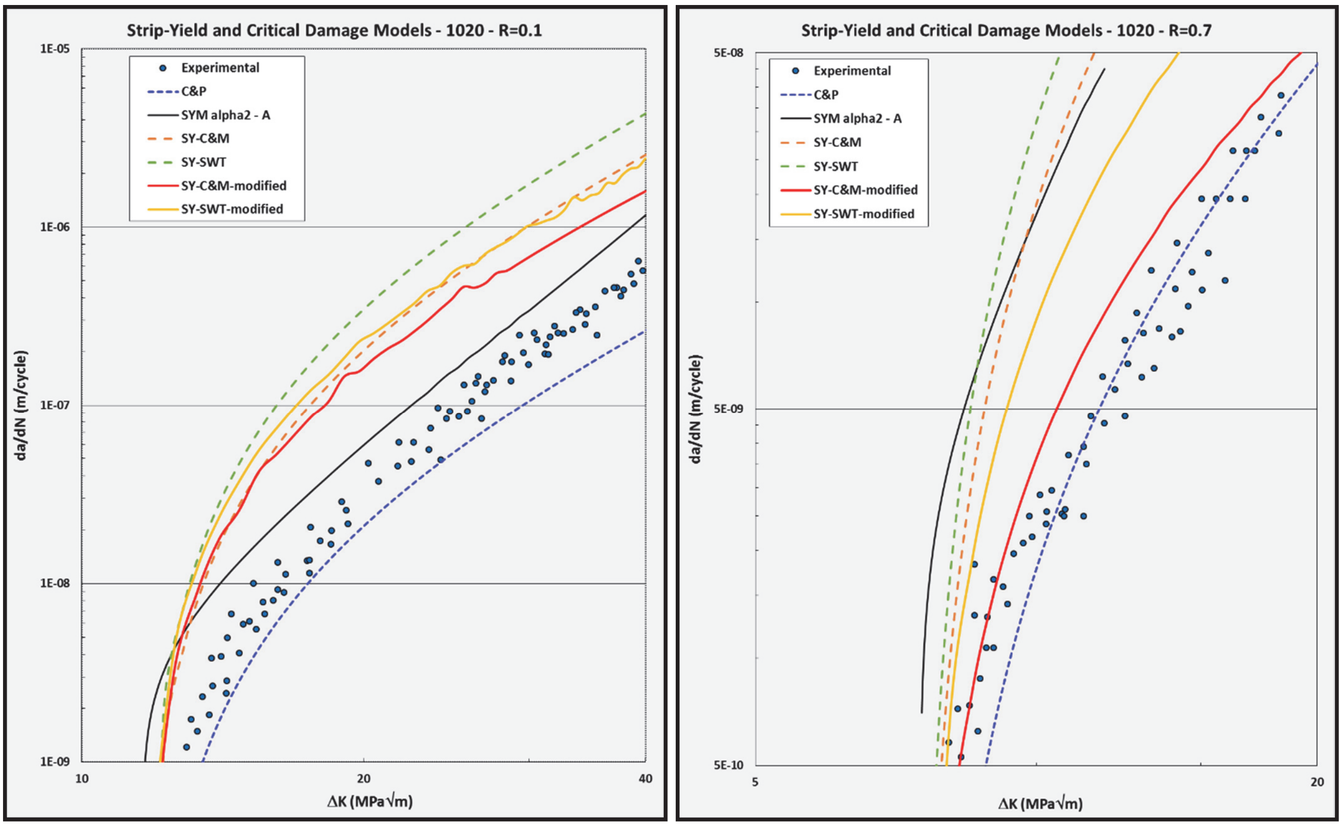

Figure 4: Strip-yield and critical damage models for the 1020 steel at R = 0.1 and 0.7.

Two facts resulting from this academic exercise must be emphasized. First, their FCG estimates were quite reasonable, an indication that their ideas about the mechanics of the FCG process probably are reasonable as well. This at least may be seen as an indication that the procedures used in these simple models are at least coherent, a reassuring evidence. However, the second fact is still more interesting, since it could not be anticipated. The study presented above show that

FCG rates estimated by opposing ideas can yield similarly reasonable results. Moreover, when the SYM and the CDM techniques are properly combined, they also generate reasonable predictions. This does not means that these methods are equivalent. Indeed, while the CDM FCG rate estimates requires only measurable εN properties and need no data-fitting parameters, the SYM estimates use at least four data-fitting parameters in a pre-chosen FCG rule to achieve similar results. This is probably not a major problem from an engineering point of view, if such parameters are available. However, it is undeniable that to generate similar descriptions of measured FCG data using only standard εN properties and basic mechanical principles is a point in favor of CDM ideas.
Finally, an additional point must be emphasized as well, although it is more philosophical than operational: the results presented here also indicate that a good description of some experimental data *cannot* be claimed as a conclusive proof of any model suitability, let alone of its prevalence. What is really important when discussing the performance of any given model is to clearly identify which set of properly measured experimental data it *cannot* describe well. This point is important, since after so many years still there is no consensus even about which are the true fatigue crack driving forces, let alone on the best FCG model. Indeed, whereas many defend that fatigue cracks are driven by ΔK_{eff}, others affirm that fatigue crack closure is not even a major issue in FCG. The authors hope this relatively straightforward modeling exercise can contribute at least to avoid the radical opinions that are still too common in this field.

CONCLUSIONS

FCG models based on critical damage and strip-yield procedures are used to estimate $da/dN \times \Delta K$ curves of two materials under low and high R-ratios. These models are based on contradictory hypotheses about the cause for the FCG behavior. Whereas the SYMs assume FCG is driven by ΔK_{eff}, so that it depends on the interference of the plastic wakes left *behind* the crack tip along the crack surfaces, the CDMs suppose fatigue cracks propagate by sequentially breaking volume elements *ahead* of the crack tip, which fail because they accumulate all the fatigue damage they could sustain.
All FCG models studied here are compared against properly measured $da/dN \times \Delta K$ curves of a 7075-T6 Al alloy and of an AISI 1020 low carbon steel, which were experimentally obtained following standard ASTM E647 procedures. Moreover, the εN properties of such materials were also measured by standard procedures, following ASTM E606 recommendations. Moreover, both the FCG and the fatigue crack initiation properties were measured in coupons machined from the same material lot, to avoid any inconsistency in the data.
Both the original CDMs (based on the HRR field displaced to eliminate the strain singularity ate the crack tip) and SYMs can describe reasonably well the measured data, even though they are apparently contradictory from a conceptual point of view. This is certainly an indication that such models are not incompatible. This claim is verified here by mixing them, using the strip yield mechanics instead of the HRR field to generate the strain field ahead of the crack tip needed for the critical damage calculations. First, this is done maintaining the hypothesis that the FCG curves can be described by McEvily's single parameter model. Then, two new hypotheses are proposed to eliminate the need for such an assumption, namely (i) there is a limit strain range related to the threshold stress intensity factor range, and (ii) there is a maximum plastic strain related to the critical stress intensity factor. These limit strain values can be introduced in the εN damage calculations, eliminating one calculation step and allowing the CDM to easier deal with variable amplitude loading problems, a feature that will be discussed in future works.
Finally, the quite reasonable performance of the predictions obtained from models based on so different hypothesis about the FCG driving forces also indicates that the good fitting of some properly obtained data set is not enough to prove which one is the best.

REFERENCES

[1] Paris, P.C., Erdogan, F. A critical analysis of crack propagation laws. J Basic Eng 85 (1963) 528-534.
[2] Castro, J.T.P., Meggiolaro, M.A., Fatigue Design Techniques, volume 3: Crack Propagation, Temperature and Statistical Effects. CreateSpace (2016).
[3] Elber, W., Fatigue crack closure under cyclic tension. Eng Fract Mech, 2 1970) 37-45.
[4] Elber, W., The significance of fatigue crack closure. Damage Tolerance in Aircraft Structures, ASTM STP, 486 (1971) 230-242.

[5] Dill, H.D., Saff, C.R., Spectrum crack growth prediction method based on crack surface displacement and contact analyses. Fatigue Crack Growth under Spectrum Loads, ASTM STP 595 (1976) 306-319.
[6] Newman, Jr, JC., A crack-closure model for predicting fatigue crack growth under aircraft spectrum loading. Methods and Models for Predicting Fatigue Crack Growth under Random Loading, ASTM STP 748 (1981) 53-84.
[7] de Koning, A.U., Liefting, G.. Analysis of crack opening behavior by application of a discretized strip yield model. Mechanics of Fatigue Crack Closure, ASTM STP 982 (1988) 437-458.
[8] Wang, G.S., Blom, A.F., A strip model for fatigue crack growth predictions under general load conditions. Eng Fract Mech, 40 (1991) 507-533.
[9] Beretta,S, Carboni,M. A strip-yield algorithm for the analysis of closure evaluation near the crack tip. Eng Fract Mech 72 (2005) 1222-1237.
[10] Kemp, P.M.J., Fatigue crack closure – a review. TR90046, Royal Aerospace Establishment, UK, (1990).
[11] Skorupa, M., Load interaction effects during fatigue crack growth under variable amplitude loading - a literature review - part I: empirical trends, Fatigue Fract Eng Mater Struct, 21 (1998) 987-1006.
[12] Skorupa, M., Load interaction effects during fatigue crack Growth under variable amplitude loading - a literature review - part II: qualitative interpretation, Fatigue Fract Eng Mater Struct, 22 (1999) 905-926.
[13] Castro, J.T.P., Meggiolaro, M.A., Miranda, A.C.O., Singular and non-singular approaches for predicting fatigue crack growth behavior. Int J Fatigue, 27 (2005) 1366-1388.
[14] Castro, J.T.P., Meggiolaro, M.A., González, J.A.O., Can ΔK_{eff} be assumed as the driving force for fatigue crack growth? Frattura ed Integrità Strutturale, 33 (2015) 97-104.
[15] Castro, J.T.P., González, J.A.O., Meggiolaro, M.A., González, G.L.G., Freire, J.L.F., Some questions about assuming ΔK_{eff} as the sole FCG driving force. Submitted to Int J Fatigue, (2016).
[16] Chen, D.L., Weiss, B., Stickler, R., The effective fatigue threshold: significance of the loading cycle below the crack opening load. Int J Fatigue, 16 (1994) 485-491.
[17] Vasudevan, A. K., Sadananda, K., Holtz, R. L., Analysis of vacuum fatigue crack growth results and its implications, International J. Fatigue, 27 (2005) 1519-1529.
[18] Castro, J.T.P., Kenedi, P.P., Prediction of fatigue crack growth rates departing from Coffin-Manson concepts. J Braz Soc Mech Sci Eng, 17 (1995) 292-303 (in Portuguese).
[19] Durán, J.A.R., Castro, J.T.P., Payão Filho, J.C., Fatigue crack propagation prediction by cyclic plasticity damage accumulation models, Fatigue Fract Eng Mater Struct, 26 (2003) 137-150.
[20] Castro, J.T.P., Meggiolaro, M.A., Miranda, A.C.O., Fatigue crack growth predictions based on damage accumulation calculations ahead of the crack tip, Comput Mat Sci, 46 (2009) 115-123.
[21] Rice, J.R., Rosengren, G.F., Plane strain deformation near a crack tip in a power-law hardening material, J Mech Phys Solids, 16 (1968) 1-12.
[22] Hutchinson, J.W., Singular behavior at the end of a tensile crack tip in a hardening material, J Mech Phys Solids 16 (1968) 13-31.
[23] Creager, M., Paris, P.C., Elastic field equations for blunt cracks with reference to stress corrosion cracking, Int J Fract Mech, 3 (1967) 247-252.
[24] Schwalbe, K.H., Comparison of several fatigue crack propagation laws with experimental results, Eng Fract Mech 6 (1974) 325-341.
[25] Dugdale, D. S., Yielding of sheets containing slits, J Mech Phys Solids, 8 (1960) 100-104.
[26] Barenblatt, G.I., The mathematical theory of equilibrium cracks in brittle fracture. Advances in Applied Mechanics, 7 (1962) 55-192.
[27] NASGRO – Fracture Mechanics and Fatigue Crack Growth Analysis Software, Reference Manual, version 4.02, (2002).
[28] Newman, J.C., FASTRAN II: a fatigue crack growth structural analysis program, NASA Technical Memorandum 104159, LRC Hampton, (1992).
[29] Newman, J.C., A Crack Opening Stress Equation for Fatigue Crack Growth. Int J Fract, 24 (1984) R131-R135.
[30] Rice, J.R., Mechanics of crack tip deformation and extension by fatigue. Fatigue Crack Propagation, ASTM STP 415 (1967) 247-311.